Oxygen-induced Decrease in the Equilibrium Adsorptive Capacities of Activated Carbons

C.O. Ania, J.B. Parra* and J.J. Pis *Instituto Nacional del Carbón (INCAR) C.S.I.C., Apartado 73, 33080 Oviedo, Spain.*

(Received 17 November 2003; revised form accepted 22 January 2004)

ABSTRACT: Special attention was paid in this work to the role of surface chemistry in the adsorption of phenol and salicylic acid onto activated carbons. To this end, two commercial activated carbons (granular and powdered) were oxidised using ammonium peroxodisulphate [$(NH_4)_2S_2O_8$] and nitric acid in different concentrations. The structural and chemical properties of the oxidised adsorbents were characterised via nitrogen adsorption isotherms measured at –196°C and Boehm titrations. Phenol adsorption from solution at low concentration was studied at room temperature without specific pH control of the solution. The results showed a significant reduction in the adsorptive capacities towards phenol of the activated carbons as the oxygen content of the latter increased. However, very little effect was observed towards the retention of salicylic acid. The decrease in adsorptive capacity depended not only on the amount of oxygen per unit mass of activated carbon, but also on the textural properties of the latter.

INTRODUCTION

To date, the active ingredients of pharmaceutical products have received little attention from the scientific community despite their extensive use all over the world. These chemical pollutants present a large number of components exhibiting great diversity in their structure and in their chemical and biochemical activities. The potential contamination of water resources by chemicals, including pharmaceuticals, is of growing concern. In this connection, the European Union (EU) is encouraging research into emerging problems such as the increasing presence of pharmaceutical residues in water and wastewater. This concern is understandable given the risk they pose to the environment and to human health [Fifth (EC) RTD Framework Programme (1998–2002)]. Until now, interest has focused mainly on veterinary antibiotics but recent studies have also reported residues of human pharmaceuticals in wastewater and the aquatic environment. Very little documentation on the environmental properties is available for the majority of pharmaceuticals and, hence, the possible impact of these residues is uncertain.

Activated carbons (ACs) are used extensively as adsorbents for decontamination processes such as the purification of drinking water (Mazyck and Cannon 2000), wastewater treatment (Walker and Weatherley 2000; Gurrath *et al*. 2000), emission control (Hadidi *et al*. 1999), etc. The treatment of industrial wastewater is one of the main areas of growth for activated carbon. This is due to increasingly stringent environmental regulation and greater emphasis on water re-utilisation, decontamination of effluents and lower disposal costs. Activated carbons are also used in purification and recovery processes in the processing of chemicals, pharmaceuticals and their

*Author to whom all correspondence should be addressed. E-mail: jbparra@incar.csic.es.

intermediates (Sircar *et al*. 1996). By adsorbing impurities in chemical processes, ACs control the quality and consistency of products. The treatment of polluted effluents from the pharmaceutical industry with ACs avoids the deposition of contaminants and makes them available for recycling. The adsorption capacity of a given AC depends on several factors such as its texture and chemical structure. The most important features of activated carbon used in water treatment are a high surface area and a wide range of pore sizes (Derbyshire *et al*. 2001). Small pores are effective in adsorbing low molecular weight compounds such as phenolics, whereas large pores are effective in adsorbing high molecular weight compounds.

There has been increasing interest in the study of the adsorption of organic molecules onto activated carbons, particularly phenol (Abuzaid and Nakhla 1994; Nevskaia *et al*. 1999; Ferro-Garcia *et al*. 1996). This is due to the importance of the removal of organic pollutants from water streams. While the issue of the textural characteristics of activated carbons has been widely studied by numerous authors (Radovic *et al*. 1995; Sircar *et al*. 1996; Moreno-Castilla and Rivera-Utrilla 1995; Bercic *et al*. 1996) and is well understood, works on elucidating the role of the oxygen surface chemistry of carbons in the process of adsorption of organic compounds have not been so successful (Vidic *et al*. 1997; Sheintcuh and Matatov-Meytal 1999; Moreno-Castilla *et al*. 1995).

Taking the above considerations into account, the aim of the present work was to study the influence of the texture and chemical properties of ACs on their adsorptive capacities towards organic compounds related to the pharmaceutical industry. This project also focused on the removal of pharmaceuticals and their metabolites from liquid effluents. The object of the study was a high-volume pharmaceutical common metabolite (salicylic acid), which is the primary hydrolytic metabolite of acetylsalicylic acid. The removal of phenol has also been investigated and compared to that of salicylic acid, as both these products are present in wastewater resulting from the industrial production of a common analgesic.

EXPERIMENTAL

Materials

Two activated carbons of coal and wood origin were used in this study. The first carbon sample was obtained by the activation of coal with water vapour and is referred to below as Q. This AC was supplied in granular form by the manufacturer and a particle size fraction of 0.212–0.075 mm was used in all the experiments. The second carbon sample, LM, was a powdered activated carbon obtained by the physical activation of wood. It was subsequently washed with hydrochloric acid to reduce the ash content. The as-received samples were previously washed several times with deionised boiling water, dried for 2 d at 110°C and stored in a desiccator until used. Both carbons were oxidised with different oxidising agents: $(NH_4)_2S_2O_8$ and HNO_3. Chemical oxidation with HNO_3 was carried out using different acid concentrations (1, 20 and 60 v/v%). The samples are referred to below by the name of the activated carbon followed by N1, N20 and N60, respectively. For treatment with HNO_3, the AC was mixed with different acid concentrations and the suspension (1 g AC/10 ml HNO_3 solution) was boiled to dryness. The resulting samples were washed thoroughly in a Soxhlet apparatus to remove excess HNO_3 and until all nitrates were eliminated. Treatment with $(NH_4)_2S_2O_8$ was as follows. The sample was treated with a saturated solution of $(NH_4)_2S_2O_8$ in 4 N sulphuric acid [1 g AC/10 ml $(NH_4)_2S_2O_8$ solution] and left overnight. The oxidised sample was washed with distilled water and dried at 110°C until no further SO_2 gas was evolved. These samples are denoted as QS and LMS.

Boehm titration and PZC

The concentrations of acid and basic groups on the carbon surface as well as their nature were determined by Boehm titration and the point of zero charge (PZC). The oxygen-containing functional groups created in the oxidised samples were determined according to the Boehm titration method (Boehm 1966). Thus, a 1-g carbon sample was placed in 50 ml of a 0.1 N solution of each of three different bases of increasing strength (NaOH, $NaHCO_3$, Na_2CO_3) and 0.1 N HCl in sealed polyethylene flasks. The suspensions were shaken overnight and then filtered. Aliquots of the filtrate were back-titrated pH-metrically with 0.1 N NaOH solution after acidification with an excess of 0.1 N HCl solution. The total number of basic sites was determined from the amount of HCl that reacted with the carbon. On the other hand, the number of different basic sites was calculated by selective neutralisation of the various surface functionalities according to their acid strength. It was assumed that $NaHCO_3$ was capable of neutralising all carboxylic groups, Na_2CO_3 the carboxylic and phenolic groups, and NaOH the carboxylic, lactonic and phenolic groups.

The PZC values were determined by mass titration as described elsewhere (Noh and Schwarz 1992). The materials were further characterised by ultimate analysis.

Textural characterisation

Textural characterisation was carried out by measuring N_2 adsorption isotherms at –196°C using an ASAP 2010 M instrument (Micromeritics Corp., Norcross, GA, USA). For such studies, samples (ca. 0.3 g) were outgassed at 150°C under vacuum for ca. 24 h. Different model methods (i.e. BET, Dubinin–Radushkevich, DFT) were applied to the N_2 adsorption isotherms in order to calculate the specific surface area, the micropore volume and the pore volume distribution (DFT). The resultant textural parameters were compared.

Phenol and salicylic acid adsorption from aqueous solution

Prior to the adsorption studies, the time necessary to attain equilibrium conditions for the uptake of both pollutants on the activated carbons was determined via kinetic studies. The equilibration period allowed was 30 and 5 d for phenol and salicylic acid, respectively. Equilibrium adsorption isotherms for the retention of phenol on the AC selected were obtained from close batch experiments under oxic conditions at 30°C using the bottle-point technique (Leng and Pinto 1997). Different amounts of AC — increasing from 20 mg up to 500 mg — were weighed accurately and placed in dark glass flasks containing 100 ml of a solution of the organic compound. The concentration range investigated extended to 250 ppm. The flasks were covered with caps and placed in a shaker at room temperature (30°C) and shaken at 100 rpm. After equilibration, the adsorbate concentration in the supernatant liquid was measured on a Shimadzu 2501 UV–vis spectrophotometer at a wavelength of 269 nm for phenol and of 256 nm for salicylic acid. The amount of adsorbate retained, q_e, was calculated from the equation:

$$q_e = \frac{V(C_0 - C_e)}{M} \quad (1)$$

where V is the volume of the liquid phase, C_0 is the initial concentration of the adsorbate solution, C_e is the concentration of the solute in the bulk phase at equilibrium and M is the amount of adsorbent employed. In addition, a blank was checked for every experiment to verify that there

was no adsorbate volatilisation or adsorption on the walls. The adsorbates used in this research were reagent grade phenol and salicylic acid. All solutions were prepared with deionised unbuffered water.

The isotherms obtained were fitted with the Freundlich isotherm (Freundlich 1926). This is an empirical relationship based on the assumption of a logarithmic decrease in the adsorption heat with surface coverage. The Freundlich equation also allows for the average of different multilayer adsorption energies and different surface adsorption energies, both of which are affected by the size and distribution of pores in an adsorbent. This equation was used in the form:

$$q = K_f \bullet C^n \quad (2)$$

where q is the amount adsorbed/g adsorbent, C is the adsorbate concentration in the liquid phase, n is an empirical parameter representing the heterogeneity of site energies and K_f is the unit capacity factor related to the adsorbent capacity.

RESULTS AND DISCUSSION

Characterisation of the porosity of the oxidised activated carbons

The detailed characteristics of the pore structure of samples Q and LM and their counterparts are listed in Table 1. Samples Q and LM differed noticeably in their pore structures; thus, for example, Q exhibited a larger surface area and micropore volume than sample LM. On the other hand, it is worth pointing out that despite its lower BET apparent surface area, sample LM had a highly developed microporosity. This was corroborated by the high value of the C_{BET} parameter and the pore volume distribution (cf. Figure 1). When applied to the nitrogen adsorption isotherms,

TABLE 1. Textural Parameters Obtained from Nitrogen Adsorption Isotherms and Chemical Properties of Samples Studied

Sample	S_{BET} (m^2/g)	C_{BET}	D–R equation				Chemical properties				PZC
			W_0 (cm^3/g)	E_0 (kJ/mol)	L (nm)	S_{mic} (m^2/g)	C (%)	H (%)	N (%)	O (%)	
Q	1149	242	0.422	18.7	1.47	572	85.6	0.5	0.6	1.9	9.2
QN1	1054	300	0.394	19.2	1.39	566	84.3	2.7	1.0	2.3	6.2
QN20	805	179	0.282	18.7	1.49	379	78.7	2.8	1.5	11.3	5.1
QN60	309	610	0.114	22.8	0.95	241	75.3	2.8	1.7	15.0	4.2
QS	1032	249	0.376	18.9	1.45	519	67.8	2.8	0.7	10.3	2.3
LM	896	727	0.345	21.39	1.08	639	93.9	0.9	0.5	3.3	8.2
LMN1	907	907	0.340	22.47	0.98	698	91.5	2.3	0.9	5.0	6.1
LMN20	874	874	0.321	21.29	1.09	588	81.3	2.5	1.5	13.2	4.5
LMN60	411	411	0.154	23.81	0.87	339	79.7	2.7	1.8	14.4	3.5
LMS	816	591	0.304	21.38	1.08	563	82.5	2.7	0.5	12.7	2.0

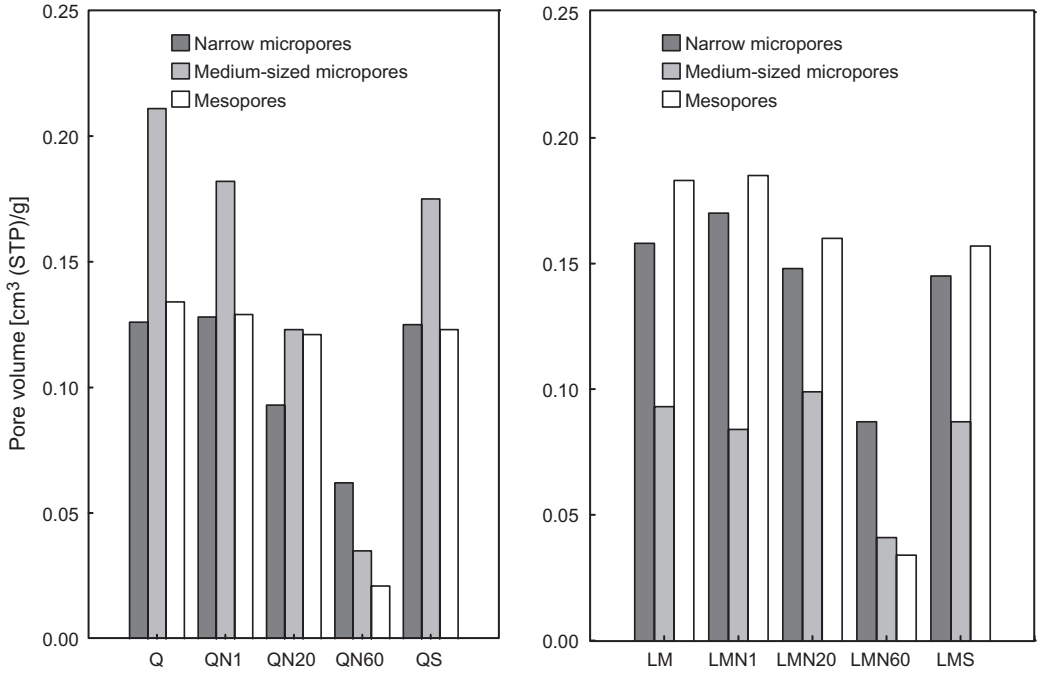

Figure 1. Pore volume distributions obtained by the application of the DFT equation to the nitrogen adsorption isotherms at –196°C for the samples studied.

the DFT model enabled the pore volume distributions to be obtained according to the IUPAC classification. In this sense, the narrow micropore volume (V_{nm}) was 1.25-times greater in the LM sample. Thus, the LM carbon had a narrow pore-size distribution as evidenced by data from gas adsorption, while sample Q showed a wider pore-size distribution.

Oxidation caused some changes in the porosities of the samples, leading to a decrease in the surface area and micropore volume for both carbons. It is worth mentioning, however, that the structural effects of oxidation were less pronounced for LM than for sample Q, and also for oxidation with $(NH_4)_2S_2O_8$ compared with HNO_3 oxidation. All the adsorption isotherms were of type I in the BDDT classification, indicating that the samples were mainly microporous. The desorption isotherms of the original and the oxidised samples showed a small hysteresis loop, indicating the existence of some mesoporosity. However, desorption isotherms for QN60 and LMN60 were reversible, indicating a decrease in the mesoporosity of these samples. Oxidation led to a downward shift of the isotherm. For oxidation with HNO_3, this shift was a maximum for QN60 and LMN60, whilst for oxidation with $(NH_4)_2S_2O_8$ and 1 v/v% HNO_3 it was a minimum. Depending on the strength of the oxidising agent, it was found that the changes in the porous structure were extremely significant. Although treatment with 1 v/v% HNO_3 and $(NH_4)_2S_2O_8$ to produce samples N1 and S caused only a tiny decrease in the porous structure of the original AC, when severe oxidation was undertaken substantial textural and chemical changes occurred.

The BET apparent surface areas decreased significantly as the concentration of HNO_3 employed for oxidation increased. On being oxidised with different oxidising agents, the surface areas of the activated carbons decreased in the order S > N1 > N20 > N60. This was due to destruction

of the sample porosity as a result of the fixation of oxygenated functional groups on the AC surfaces. It is thought that the oxygen was mainly fixed at the pore entrances, thereby increasing their constriction and preventing the total pore structure of the sample from being accessed by nitrogen gas. Thus, for example, the BET apparent surface area of QN60 was nearly four-times lower than that of Q. Moreover, the C_{BET} value of QN60 was surprisingly the highest, indicating that the sample had become the most microporous of the modified adsorbents.

Application of the Dubinin–Radushkevitch equation showed a simultaneous decrease in the micropore volumes of samples subjected to oxidation. This was visible from the magnitudes of the quantity W_0 associated with this equation. There was also a narrowing of microporosity in samples QN60 and LMN60 as shown by an increase in E_0, and hence a decrease in the L value calculated from the Stoeckli–Ballerini equation (Stoeckli and Ballerini 1991). This parameter is a measure of accessible pore width. A narrowing of the micropore distribution was observed when activated carbon was oxidised with 60 v/v% HNO_3. This finding is in good agreement with the high C_{BET} value found for this sample, suggesting that the microporosity in this material was mainly composed of narrower pores than that in samples N1, N20 or S.

The pore volume distribution (cf. Figure 1) can be obtained by applying the DFT model to the nitrogen adsorption isotherms. From this it was observed that the microporosity and mesoporosity of the oxidised samples decreased with the increasing HNO_3 concentration, while QS and LMS showed textural characteristics close to those of samples QN1 and LMN1, respectively. Despite their low apparent surface area, QN60 and LMN60 show relatively large volumes associated with narrow microporosity, indicating that oxidation completely destroyed the medium-sized micropores and mesopores of a larger size. Thus, the porosity of these samples was mainly associated with smaller-sized pores. This may be due to diffusion of the oxidising agent from the liquid phase through the porous structure of the carbon particle. The kinetics of diffusion into a structure containing narrow micropores would be slower due to the limited size of these pores, so that oxidation may have occurred mainly in the most accessible pore structure of the carbon, particularly in pores of a larger diameter.

The decrease in the BET surface area and the destruction of the pore structure brought about by strong oxidants may also be attributed to the destruction of the pore walls (Moreno-Castilla *et al*. 1998). At high concentrations, the application of HNO_3 destroys the pores. Moreover the pore walls may collapse when oxygenated terminal groups are created. From this it may be inferred that, as far as oxidation is concerned, changes to the physical morphology of the AC would depend on the strength of the oxidising agent and the operating conditions. In summary, severe oxidation at extreme conditions virtually destroyed the porous structure of the original AC due to erosion of the pore walls, while oxidation carried out under moderate conditions brought about slight modification in the original textural characteristics.

Scanning electron microscope (SEM) studies of the samples concerned corroborated this suggestion. Thus, examination of the SEM micrographs of the oxidised carbons (cf. Figure 2) shows significant changes in the physical morphology of the adsorbents. These modifications were greater as the concentration of the HNO_3 employed increased. Oxidation with high HNO_3 concentrations led to the progressive formation of particle aggregates, thereby drastically modifying the carbonaceous structure of the initial adsorbent. On the other hand, micrographs of samples oxidised with $(NH_4)_2S_2O_8$ showed a certain degree of wall alteration, although this modification was not as great as in samples treated with HNO_3. This suggests that $(NH_4)_2S_2O_8$ oxidation, although as strong as treatment with HNO_3 (cf. Table 1), preserved the physical morphology of the activated carbon.

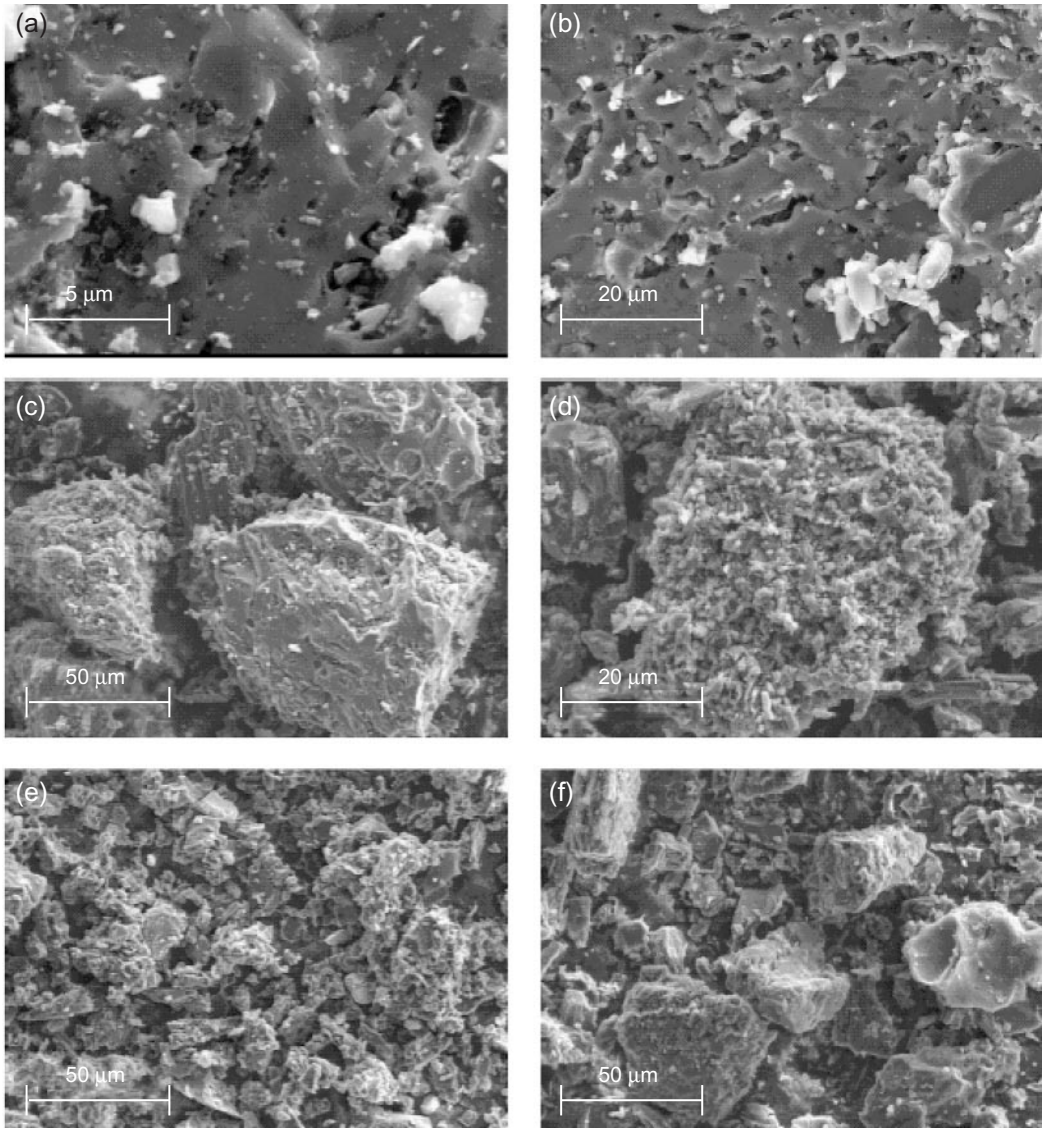

Figure 2. SEM micrographs of (a) the original sample Q and of the oxidised samples (b) QN1, (c) QN20, (d) QN60 (20 µm magnification), (e) QN60 (50 µm magnification) and (f) QS.

Characterisation of surface functionalities

The main purpose of oxidation is the creation of functionalities on the surface of the adsorbent. Ultimate analysis of the samples studied showed a significant increase in their oxygen content with increasing concentration of the HNO_3 solutions employed (cf. data listed in Table 1). The nitrogen content of samples oxidised with HNO_3 increased slightly with increasing HNO_3

concentration, whereas the oxygen content increase was considerable. These results suggest that nitrogen functionalities were created at low HNO_3 concentration and thus the functional groups created on the surface of the activated carbons were mainly oxygenated.

Depending on the strength of the oxidising agent, considerable changes occurred in the chemical properties of the ACs. Treatment with HNO_3 at high concentrations to produce the N20 and N60 samples gave rise to a large increase in oxygen content. On the other hand, oxidation by $(NH_4)_2S_2O_8$ led to an increasingly high oxygen content in the samples, close to that achieved via 20 v/v% HNO_3. It is well known that the acidic nature of ACs is closely related to their oxygen content. Accordingly, the PZC values should show a corresponding increase in the acidic nature of the oxidised samples. Initially, due to their low oxygen content, the as-received samples Q and LM presented a basic nature. After oxidation with HNO_3 at a low concentration, QN1 and LMN1 exhibited a lower PZC although they remained basic carbons to all intents and purposes. However, samples N20, N60 and S presented even lower PZC values, due to the large amount of oxygenated functional groups created on their surfaces.

According to the method proposed by Boehm, the functionalities created on the surface of activated carbons can be identified and quantified. Table 2 presents the Boehm titration results obtained in the present studies where the amount of groups present is reported in terms of surface concentration (μequiv/g). A significant increase in the number of acidic groups occurred for both carbons after oxidation, along with a decrease in the number of basic groups. From the total content of acidic and basic groups, it can be inferred that the overall effect of oxidation was slightly more evident for sample LM relative to Q. Although the former exhibited a somewhat smaller content of oxygenated functional groups (either basic or acidic), its oxidised samples showed a relatively larger amount of acidic groups.

Samples QS and LMS possessed lower concentrations of carboxylic groups compared to samples oxidised with 60 v/v% HNO_3. However, the use of $(NH_4)_2S_2O_8$ led to the formation of a larger number of lactonic groups. Oxidation with low HNO_3 concentrations did not lead to significant changes either in the porous structure or in the surface chemistry of the samples. However, $(NH_4)_2S_2O_8$ gave rise to considerable oxidation as demonstrated by the large oxygen content and the Boehm titration results, without much alteration in the porous characteristics of the raw activated carbons.

TABLE 2. Results of Boehm Titrations for Samples[a]

Sample	Carboxylic	Lactonic	Phenolic	Total acidic	Basic	All
Q	0	110	–	110	442	552
QN1	0	94	45	139	240	379
QN20	122	239	54	415	172	587
QN60	698	37	763	1498	0	1498
QS	364	305	495	1164	0	1164
LM	0	162	–	162	310	472
LMN1	0	142	–	142	150	292
LMN20	148	350	63	561	105	666
LMN60	715	44	786	1545	0	1545
LMS	385	405	527	1317	0	1317

[a]All values quoted in μequiv/g.

Adsorption of organic compounds from the liquid phase

Isotherms of phenol and salicylic acid on the original and oxidised samples, together with the corresponding fits of the Freundlich equation, are presented in Figure 3. With phenol, its retention in samples Q and LM was comparable. Despite the low surface area and the relatively low micropore volume (cf. Table 1) of sample LM, the phenol uptake was similar to that attained in Q, suggesting that the porosity and textural properties of the samples did not contribute to phenol retention. Thus, as expected, the adsorptive capacities towards phenol must be explained in terms of the chemical properties of each activated carbon. From the results of the Boehm titration, both samples presented equivalent amounts of basic and acidic groups, and similar PZC and oxygen content values. This result was in good agreement with the similar phenol uptake of both samples.

As far as the isotherm shapes and their initial slopes are concerned, all belonged to type L in the Giles classification (Giles *et al*. 1960). A concavity relative to the abscissa was displayed in all cases, indicating that as more sites in the substrate were filled it became increasingly difficult for a bombarding solute molecule to find an available vacant site. This implies either that the adsorbed solute molecule was not oriented vertically or that there was no strong competition for the solvent. The phenol adsorption isotherms showed a plateau value at high adsorbate concentrations (subgroups 1 and 2), suggesting that the sorbate uptake proceeded via monolayer complexion. The development of a second layer was not observed in any cases of phenol retention.

Previous studies have shown that phenol adsorption is dependent on both the texture and the presence of surface functional groups in carbons (Radovic *et al*. 1995; Magne and Walker 1996; Mahagan *et al*. 1980). However, our results did not show any direct correlation between the uptake of phenol and any of the textural properties of the carbon (i.e. BET area, micropore volume, pore width, etc.) in the as-received samples. As has been established previously, the surface chemistry of the carbon plays an important role in phenol adsorption on activated carbons (Mahagan *et al*. 1980). The mechanism of adsorption may imply electron donor–acceptor complexes or may involve dispersion forces between the π-electrons of the adsorbate and the basal planes of the carbon. Taking these considerations together with the characterisation of the functional groups on samples Q and LM into account, phenol uptake on these samples must have been due to both mechanisms. Thus, the basic surface oxygen groups present in both carbons acted as donors while the aromatic ring of the phenol molecule acted as an acceptor. In addition, dispersive interactions were promoted between the basal planes of the graphene layers and the π-electron density of the aromatic ring of phenol.

In agreement with the observations of other workers (Nevskaia *et al*. 1999; Moreno-Castilla *et al*. 1995; Mahagan *et al*. 1980), the uptake of phenol decreased on the oxidised samples of both carbons studied here. This decrease in uptake compared to the initial samples was greater for LM than for Q, although oxidation on sample Q gave rise to a greater destruction of the porous structure of the sample. Secondly, in the case of LM, the effect of oxidation appeared to be more pronounced than for Q from a chemical point of view (cf. Table 1). Thus, the results of the Boehm titrations showed a greater number of acidic groups per g carbon recorded on counterparts of sample LM. Hence, the decrease in the phenol uptake on samples of the LM series was basically due to chemical changes.

When oxidation occurs, additional oxygen functional groups are created on the carbon surface, and the decrease in phenol uptake observed must be due to several factors. According to the Boehm results, oxidation created functionalities of an acidic nature. Since the adsorption of phenol requires the presence of basic surface groups, a weakening in the donor–acceptor complex mechanism would be expected under these circumstances.

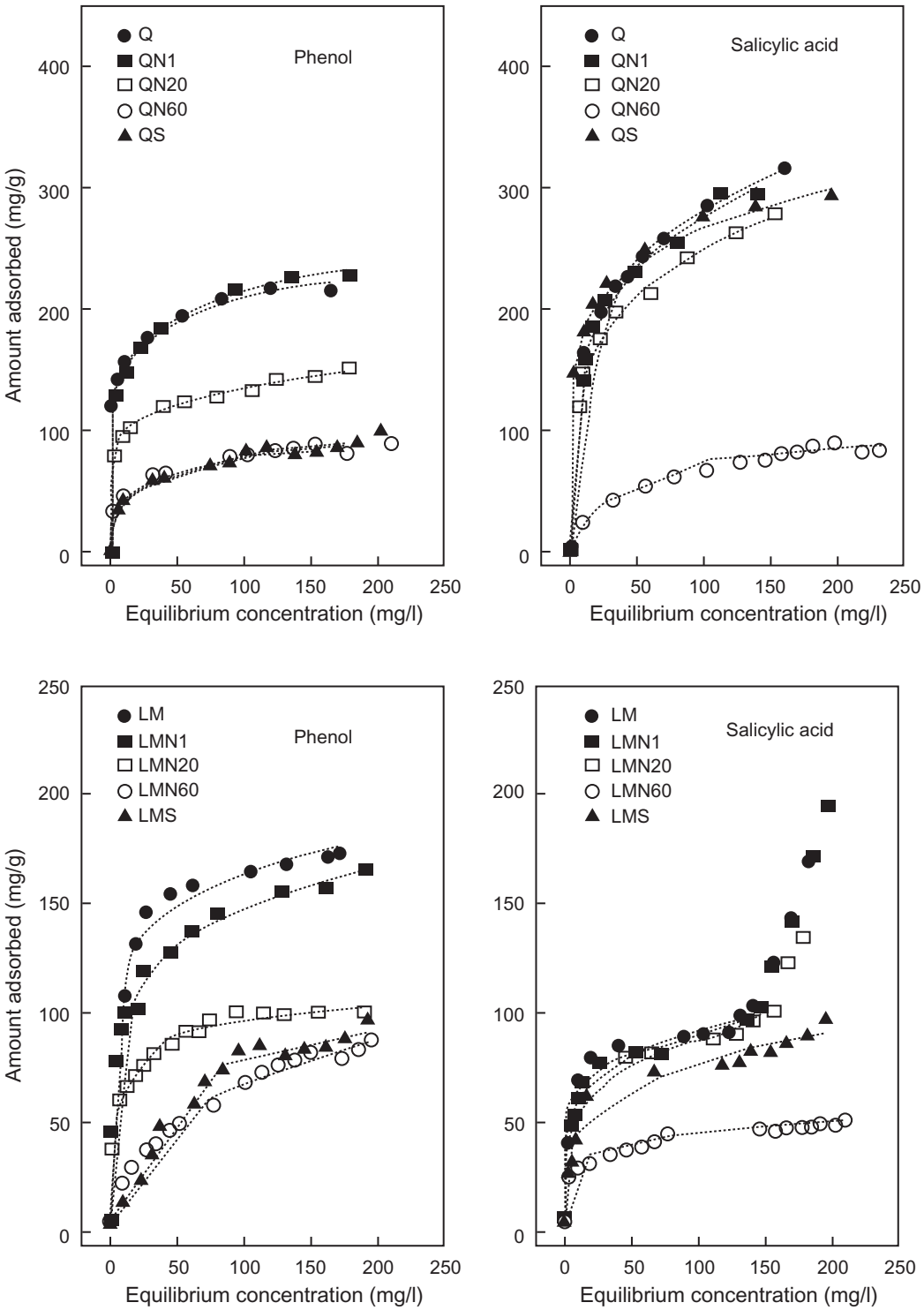

Figure 3. Liquid-phase equilibrium adsorption isotherms for phenol and salicylic acid onto the activated carbons studied (symbols) and the various fits to the Freundlich equation (dotted lines).

In addition, dispersive interactions were also found to weaken. To examine this point, the experimental cross-sectional area of phenol was calculated from the experimental adsorption data for the oxidised samples and compared with the theoretical value (σ = 52.2 Å^2) (Puri *et al*. 1972). It was found that the phenol molecules did not cover the entire surface for the untreated activated carbons (coverage degree values of up to 65%). This value decreased to 40% for the oxidised samples of both series. A decrease in the carbon surface coverage of the oxidised samples corroborates the view that oxidation gave rise to a decrease in the π-electron density on the carbon surface, and consequently, to a diminution of adsorption produced by dispersive interactions. The functionalisation of the carbon surface with electron-acceptor groups (i.e. carboxylic and phenolic groups) would lead to a withdrawal of π-electron density from the graphene layers of the basal planes. This would cause a decrease in the strength of the dispersive interactions so that fewer phenol molecules would cover the carbon surface.

The salicylic acid adsorption isotherms also belonged to the L type, although the data obtained showed differences in uptake for samples Q and LM. The different shapes of the isotherms for salicylic acid compared with those obtained with phenol suggests that adsorption occurred via different pathways in these two cases. Salicylic acid retention on the series Q samples belonged to subgroup 1, as completion of the monolayer was not observed in all cases. However, with samples LM, LMN1 and LMN20, a remarkable increase in slope was observed at high concentrations, indicating that adsorption occurred via a second layer. Lower salicylic acid concentrations were only capable of displacing adsorbed water from a carbon surface free from functional groups up to the first plateau in the isotherm was reached. However, when a sufficient concentration of adsorbate molecules was present, the salicylic acid molecules displaced water bound to oxygenated functional groups and formed the second plateau in the isotherm.

The significantly larger uptake of salicylic acid for Q compared to LM can be explained in terms of differences in the porosities and surface areas of these samples. Both ACs exhibited a basic nature and similar surface functionalities. The main differences were the low apparent BET surface area of LM compared to Q and the micropore volumes. Despite its large narrow micropore volume, carbon LM possessed only poorly developed medium-sized microporosity, suggesting that these pores played an important role in the adsorption of each organic compound. On the other hand, diffusion of the adsorbate from the solution to the microporous structure of the samples was favoured in all cases by the high mesoporosity of the activated carbons. Thus, the low retention exhibited by carbon LM may be due to the lack of a microporous structure of an adequate size. These results suggest that the retention of salicylic acid was mainly due to physisorption on the textural matrix.

However, a different type of salicylic acid adsorption was observed on the oxidised samples. In this case, the uptake was higher in carbons with a highly developed porous structure, regardless of their acidic/basic natures. For instance, QS and LMS retained almost the same amount of salicylic acid as either Q or QN1; despite being oxidised carbons, both retained much more salicylic acid than samples oxidised with HNO_3 at a high concentration (cf. Figure 3). It seems that the changes induced in surface chemistry after oxidation did not have a significant influence on the adsorptive capacities towards salicylic acid. This suggests that adsorption of this compound was more closely related to the textural characteristics of the carbon rather than to its surface chemistry. In both oxidised series (Q and LM), good correlations were attained between the adsorption of salicylic acid and the textural properties of the activated samples (Figure 4). However, no agreement at all was found regarding the functional groups created after oxidative treatment.

The adsorption of salicylic acid could have occurred via two pathways: physisorption and chemisorption. Physisorption of the adsorbate onto the porous structure of the activated carbon is

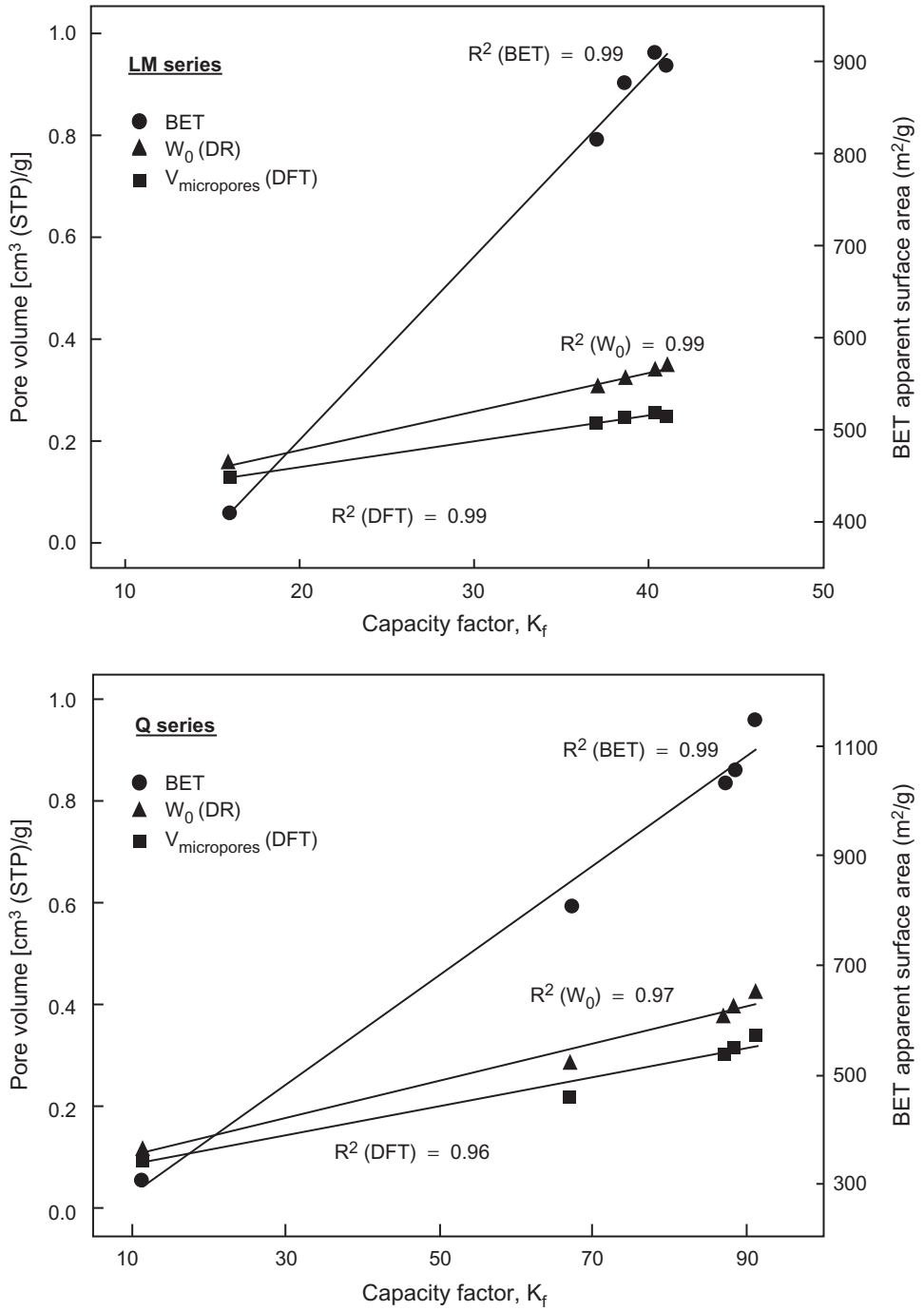

Figure 4. Correlation between the K_f parameter of the Freundlich equation and the textural properties of the various carbon samples studied.

suggested by the correlation found between the retention and textural parameters, as mentioned above. Furthermore, a chemisorption contribution to the total adsorption process would not be unexpected.

It might be thought that, despite the withdrawal effect, the functionality of salicylic acid could have been responsible for repulsive/attractive electrostatic interactions with the oxygenated functional groups created on the surfaces of the oxidised samples. However, no evidence for this fact was found. Electrostatic interactions would cause a different behaviour in oxidised samples towards the uptake of salicylic acid, but there was no evidence for this. The only correlation was a drop in the retention of salicylic acid as a consequence of the destruction of the porous structure of the carbon during the oxidative treatment.

In addition, dispersive interactions were weakened due to the functionalities associated with the molecule. The presence of the carboxylic group in the salicylic acid molecule would lead to a withdrawal of π-electron density from the aromatic ring, since the latter constitutes an electron-acceptor group in itself. As the electronic density decreased in the adsorbate aromatic ring, the strength of dispersive interactions capable of promoting adsorption also decreased. However, the adsorption of salicylic acid was still greater than the corresponding retention of phenol. This can be attributed to the chemical nature of the adsorbate. As far as the chemical structure is concerned, both phenol and salicylic acid are organic compounds with different solubilities and aromatic ring functionalities. The solubility of phenol in water is greater (6.7 g/l) than that of salicylic acid (2 g/l), so that it is more readily retained on the adsorbent.

Table 3 provides a compilation of the Freundlich parameters obtained from fitting the experimental data to the model equation. Data corresponding to second-layer adsorption coverage was not included in the fitting, as the Freundlich equation does not consider that such coverage approaches a constant value (i.e. completion of a monolayer is only considered) (Freundlich 1926). The linear range and the correlation coefficients for the Freundlich model are also listed in the table. It will be observed that this equation was capable of fitting the adsorption data at low concentrations.

TABLE 3. Freundlich Adsorption Parameters, Linear Range and Linear Correlation Coefficient

Sample	Phenol					Salicylic acid				
	K_f	n	R^2	Range (ppm)		K_f	n_f	R^2	Range (ppm)	
				Fitted	Studied				Fitted	Studied
Q	110	0.140	0.9851	200–5	0–250	91	0.245	0.9973	160–5	0–250
QN1	106	0.151	0.9938	175–5	0–250	88	0.249	0.9707	140–5	0–250
QN20	53	0.203	0.9753	150–35	0–250	68	0.269	0.9796	150–5	0–250
QN60	29	0.222	0.9985	140–5	0–250	11	0.390	0.9271	150–5	0–250
QS	29	0.214	0.9990	100–5	0–250	87	0.245	0.9980	150–5	0–250
LM	110	0.087	0.9968	200–5	0–250	41	0.172	0.9523	200–5	0–250
LMN1	60	0.193	0.9962	200–5	0–250	40	0.172	0.9540	150–5	0–250
LMN20	39	0.196	0.9971	95–5	0–250	39	0.175	0.9685	150–10	0–250
LMN60	7	0.496	0.9998	80–5	0–250	16	0.203	0.9897	170–20	0–250
LMS	17	0.351	0.9923	70–5	0–250	37	0.179	0.9977	200–5	0–250

The data also show a decrease in the K_f values and an increase in the n values for the oxidised samples relative to those for the untreated activated carbons. For phenol retention, the decrease in the unit capacity factor could be taken to be a consequence of the increase in the amount of acidic functional groups on the sample surfaces together with a decrease in the micropore volume. However, our results did not show any direct correlation between the phenol uptake and any of the textural or chemical properties of the carbons (i.e. BET apparent surface area, micropore volume, pore width, amount of carboxylic groups, etc.). Nevertheless, good correlations were found for the unit capacity factor of salicylic acid and some textural parameters such as BET apparent surface area and the micropore volumes of the samples studied (Figure 4).

These results corroborate the hypothesis that physisorption was the main mechanism for the adsorption of salicylic acid on activated carbon. In fact, the experimental data confirm the importance of the porous structure of the carbon material in the adsorption of this compound, as opposed to the creation of oxygenated functional groups brought about by oxidation. The changes induced in the surface chemistry of the carbons after various oxidation treatments did not seem to play a significant role in the uptake of salicylic acid.

CONCLUSIONS

Our results indicate that oxidation of AC induced not only substantial changes in the chemistry of the samples studied, but also important modifications in the textures of the materials. Some authors have found that although treatment with HNO_3 did not affect the physical morphology of the activated carbons substantially, it altered their surface chemistries. In the present work, it was found that the physical morphologies of the ACs were also affected by the strength of the oxidising agent and the operating conditions employed. Severe oxidation under extreme conditions virtually destroyed the porous structure of the original AC due to the erosion of the pore walls. However, oxidation under moderate conditions caused only slight modifications in the original textural characteristics. In contrast, although the use of $(NH_4)_2S_2O_8$ gave rise to extensive oxidation (as evidenced by the large oxygen content and the Boehm titration data), the porous structure of the original materials was preserved.

Phenol retention was found to depend both on the surface chemistry of the activated carbon and on its porosity. Oxidation resulted in a decrease in the phenol uptake due to a combination of two factors: the creation of acidic functional groups on the carbon surface and the destruction of the porosity of the samples. However, our results showed no direct correlation between the uptake of phenol and any of the textural properties of the carbon (i.e. BET apparent surface area, micropore volume, pore width, etc.) in the as-received samples.

For salicylic acid adsorption, the results obtained indicated that uptake of the adsorbate was more related to the texture of the activated carbon rather than its surface chemistry. The changes induced in the surface chemistry of the adsorbent after oxidative treatment seemed not to play a significant role in the uptake of salicylic acid. However, good correlations were found for salicylic acid between the unit capacity factor of the Freundlich equation and some textural parameters such as BET apparent surface area and micropore volumes. These results corroborate the hypothesis that physisorption was the main adsorption mechanism for salicylic acid onto activated carbon.

Although an acceptable interpretation of our findings was not straightforward, the presence of an electron-withdrawing functional group in the adsorbate seemed to account for the disappearance of dispersive interactions between the π-electron density of the carbon surface and the aromatic ring of phenolic compounds. However, further work is needed for a complete understanding of the mechanism of salicylic acid adsorption on activated carbons.

ACKNOWLEDGEMENTS

The authors wish to thank the European Commission and the Spanish Ministry of Science and Technology (Research Project 1FD 1997-0400-CO2-01) for financial support. The SEM micrographs were obtained with the help of D. Álvarez (INCAR-CSIC, Spain).

REFERENCES

Abuzaid, N.S. and Nakhla, G.F. (1994) *Environ. Sci. Technol*. **28,** 216.
Bercic, G., Pintar, A. and Levec, J. (1996) *Ind. Eng. Chem., Res*. **35,** 4619.
Boehm, H.P. (1966) *Adv. Catal*. **16,** 179.
Derbyshire, F., Jagtoyen, M., Andrews, R., Rao, A., Martin-Gullon, I. and Grulke, E.A. (2001) *Chem. Phys. Carbon* **27,** 1.
Ferro-García, M.A., Rivera-Utrilla, J., Bautista-Toledo, I. and Moreno-Castilla, C. (1996) *J. Chem. Technol. Biotechnol*. **67,** 83.
Fifth (EC) RTD Framework Programme (1998–2002) *Energy, Environment and Sustainable Development (EESD)*, The European Commission, Brussels, Belgium: website: https://www.cordis.lu/eesd.
Freundlich, H. (1926) *Colloid and Capillary Chemistry*, Methuen & Co., London.
Giles, C., McEwan, T., Nakhwa, S. and Smith, D. (1960) *J. Chem. Soc*. 3973.
Gurrath, M., Kuretzky, T., Boehm, H.P., Okhlopkova, L.B., Lisitsyn, A.S. and Likholobov, V.A. (2000) *Carbon* **38,** 1241.
Hadidi, K., Cohn, D.R., Vitale, S. and Bromberg, L. (1999) *J. Air Waste Manage. Assoc*. **49,** 225.
Leng, C.C. and Pinto, N.G. (1997) *Carbon* **35,** 1375.
Magne, P. and Walker, Jr., P.L. (1996) *Carbon* **24,** 101.
Mahagan, O.P., Moreno-Castilla, C. and Walker, Jr., P.L. (1980) *Sep. Sci. Technol*. **18,** 1733.
Mazyck, D.W. and Cannon, F.S. (2000) *Carbon* **38,** 1785.
Moreno-Castilla, C. and Rivera-Utrilla, J. (1995) *Carbon* **33,** 845.
Moreno-Castilla, C., Carrasco-Marín, F., Maldonado-Hódar, F.J. and Rivera-Utrilla, J. (1998) *Carbon* **36,** 145.
Moreno-Castilla, C., Rivera-Utrilla, J., Joly, J.P., López-Ramón, M.V., Ferro-García, M.A. and Carrasco-Marín, F. (1995) *Carbon* **33,** 1417.
Nevskaia, D.M., Santianes, A., Muñoz, V. and Guerrero-Ruiz, A. (1999) *Carbon* **37,** 1065.
Noh, J.S. and Schwarz, A. (1992) *J. Colloid Interface Sci*. **142,** 233.
Puri, B.R., Singh, D.D. and Kaistha, B.C. (1972) *Carbon* **10,** 481.
Radovic, L.R., Silva, I.F., Ume, J.I., Menéndez, J.A., León y León, C. and Scaroni, A.W. (1995) *Carbon* **35,** 1339.
Sheintcuh, M. and Matatov-Meytal, Y.I. (1999) *Catal. Today* **53,** 73.
Sircar, S., Golden, T.C. and Rao, M.B. (1996) *Carbon* **34,** 1.
Stoeckli, H.F. and Ballerini, L. (1991) *Fuel* **70,** 557.
Vidic, R.D., Tessmer, C.H. and Uranowski, L.J. (1997) *Carbon* **35,** 1349.
Walker, G.M. and Weatherley, L.R. (2000) *Sep. Sci. Technol*. **35,** 1329.